

Supporting Information

Self-Assembly and Luminescence of Trinuclear Lanthanide Circular Helicates

Feifan Chang, Fan-da Feng, Jiao Geng and Wei Huang*

EXPERIMENTAL SECTION

Materials. Unless otherwise specified, solvents of analytical grade were purchased directly from commercial sources and used without any further purification. Dialdehyde H₂pdd was prepared via our previously reported method.¹

Experimental Methods. High resolution electrospray ionization mass spectrometry (HR-ESI-MS) was obtained using a Thermoscientific Q Exactive mass spectrometer. Powder X-ray diffraction (PXRD) measurements were performed on a Philips X'pert MPD Pro X-ray diffractometer using Cu $K\alpha$ radiation ($\lambda = 0.15418$ nm), in which the X-ray tube was operated at 40 kV and 40 mA at R.T. UV-vis spectra were recorded with a Shimadzu UV-3150 double-beam spectrophotometer using a quartz glass cell with a path length of 10 mm, and 3D fluorescence spectrometer Horiba Fluorolog-3 was utilized to study emission spectra. Unless otherwise specified, all experiments have been carried out at room temperature (298 K). Fluorescence quantum yields Φ of complexes **1-Sm** and **1-Eu** were measured using photometric integrating sphere, while Φ of complexes **1-Nd** and **1-Yb** were measured using the Yb^{III} complex of tropolone as the standard due to the limitation of our equipment. The fluorescence lifetimes were determined from time-resolved intensity decay by the method of time correlated single-photon counting (TCSPC) using a diode laser at 374 nm as the light source (Model: FL-1057), and analyzed using HORIBA Scientific DAS6 v6.8 software.

Synthesis of 1-Nd. H₂pdd (0.046 g, 0.10 mmol), NdCl₃·6H₂O (0.018 g, 0.05 mmol) and 1,3-propanediamine (0.004 g, 0.05 mmol) were dissolved in acetonitrile (20 mL) and refluxed under 90 °C in a 50 mL round-bottom flask. After being refluxed for 2 h, the reaction mixture was cooled to the R.T. and filtered. The filtrate was concentrated to obtain compound **1-Nd**. Yield: 0.038 g (67.2 %). HR-ESI-MS (positive mode, *m/z*): 1096.1247, [Nd₃L₃]³⁺.

Synthesis of 1-Sm. The synthetic process of **1-Sm** is the same as that of **1-Nd** except that SmCl₃·6H₂O (0.018 g, 0.05 mmol) was used. Yield: 72 %, (0.041 g). HR-ESI-MS (positive mode, *m/z*): 1103.1339, [Sm₃L₃]³⁺.

Synthesis of 1-Eu. The synthetic process of **1-Eu** is the same as that of **1-Nd** except that EuCl₃·6H₂O (0.018 g, 0.05 mmol) was used. Yield: 67.6 %, (0.039 g). HR-ESI-MS (positive mode, *m/z*): 1105.1338, [Eu₃L₃]³⁺. Light yellow crystals of complex **1-Eu** were obtained by slow evaporation of a mixture of ethanol/acetonitrile solution (v/v = 4:1) in air at room temperature for two weeks.

Synthesis of 1-Gd. The synthetic process of **1-Gd** is the same as that of **1-Nd** except that GdCl₃·6H₂O (0.019 g, 0.05 mmol) was used. Yield: 70 %, (0.041 g). HR-ESI-MS (positive mode, *m/z*): 1110.1390, [Gd₃L₃]³⁺.

Synthesis of 1-Dy. The synthetic process of **1-Dy** is the same as that of **1-Nd** except that DyCl₃·6H₂O (0.018 g, 0.05 mmol) was used. Yield: 80.6 %, (0.047 g). HR-ESI-MS (positive mode, *m/z*): 1115.1425, [Dy₃L₃]³⁺. Light yellow crystals of complex **1-Dy** were obtained by slow evaporation of the methanol solution in air at room temperature for two weeks.

Synthesis of 1-Er. The synthetic process of **1-Er** is the same as that of **1-Nd** except that ErCl₃·6H₂O (0.019 g, 0.05 mmol) was used. Yield: 78 %, (0.046 g). ESI-MS (positive mode, *m/z*): 1120.1466, [Er₃L₃]³⁺. Light yellow crystals of complex **1-Er**

were obtained by slow evaporation of a mixture of ethanol/acetonitrile solution (v/v = 4:1) in air at room temperature for two weeks.

Synthesis of **1-Yb.** The synthetic process of **1-Yb** is the same as that of **1-Nd** except that $\text{YbCl}_3 \cdot 6\text{H}_2\text{O}$ (0.019 g, 0.05 mmol) was used. Yield: 71.5 %, (0.042 g). HR-ESI-MS (positive mode, *m/z*): 1136.1525, $[\text{Yb}_3\text{L}_3]^{3+}$.

X-Ray Data Collection and Structural Determination. Single-crystal samples of three lanthanide helicates were covered with glue and mounted on glass fibers and then used for data collection. Crystallographic data were collected on a Bruker SMART 1K CCD diffractometer, using graphite mono-chromated $\text{MoK}\alpha$ radiation ($\lambda = 0.71073 \text{ \AA}$). The crystal systems were determined by Laue symmetry and the space groups were assigned based on systematic absences using XPREP. Absorption corrections were performed to all data and the structures were solved by direct methods and refined by full-matrix least-squares method on F_{obs}^2 by using the SHELXTL-PC software package.² All non-H atoms were anisotropically refined and all hydrogen atoms were inserted in the calculated positions assigned fixed isotropic thermal parameters and allowed to ride on their respective parent atoms. The summary of the crystal data, experimental details and refinement results for three compounds is listed in Table S1, whereas bond distances and angles are given in Table S2. In addition, hydrogen-bonding parameters are tabulated in Table S3.

References

1. K. Zhang, C. Jin, H. Q. Chen, G. Yin and W. Huang, *Chem Asian J*, 2014, **9**, 2534–2541.
2. Sheldrick, G. M. SHELXTL (Version 6.10). Software Reference Manual; Madison, Wisconsin (USA): Bruker AXS, Inc.: 2000.

Table S1. Crystal data and structural refinements for helicates **1-Eu**, **1-Dy** and **1-Er**.

	1-Eu	1-Dy	1-Er
Empirical formula	C ₁₅₃ H ₁₃₈ Cl ₁₅ N ₁₂ O ₁₈ Eu ₃	C ₁₅₃ H ₁₃₆ Cl ₁₇ N ₁₂ O ₁₈ Dy ₃	C ₁₅₃ H ₁₃₆ Cl ₁₇ N ₁₂ O ₁₈ Er ₃
Formula weight	3420.38	3520.88	3535.16
Temperature / K	150(2)	150(2)	150(2)
Wavelength / Å	0.71073	0.71073	0.71073
Crystal Size (mm)	0.12×0.10×0.10	0.12×0.10×0.10	0.12×0.10×0.10
Crystal system	Triclinic	Monoclinic	Monoclinic
Space group	P 1	C2/c	C2/c
<i>a</i> / Å	18.132(1)	18.123(1)	18.542(5)
<i>b</i> / Å	21.885(1)	30.545(2)	30.471(9)
<i>c</i> / Å	25.270(1)	30.180(2)	29.708(8)
α / °	95.683(1)	90	90
β / °	101.870(1)	90.089(1)	90.151(7)
γ / °	101.275(1)	90	90
<i>V</i> / Å ³	9521.6(6)	16706.2(18)	16785(8)
<i>Z</i> / <i>D</i> _{calcd} (g / cm ³)	2 / 1.193	4 / 1.400	4 / 1.399
<i>F</i> (000)	3456	7076	2936
μ / mm ⁻¹	1.240	1.661	7100
<i>h</i> _{min} / <i>h</i> _{max}	-21 / 21	-21 / 21	-22 / 20
<i>k</i> _{min} / <i>k</i> _{max}	-26 / 23	-36 / 35	-36 / 35
<i>l</i> _{min} / <i>l</i> _{max}	-30 / 30	-25 / 35	-35 / 35
Data / parameters	33324 / 1810	14710 / 910	14776 / 910
	<i>R</i> ₁ = 0.0626	<i>R</i> ₁ = 0.0710	<i>R</i> ₁ = 0.0600
<i>R</i> ₁ , <i>wR</i> ₂ [<i>I</i> > 2σ(<i>I</i>)]	<i>wR</i> ₂ = 0.1698	<i>wR</i> ₂ = 0.1720	<i>wR</i> ₂ = 0.1538
	<i>R</i> ₁ = 0.0891	<i>R</i> ₁ = 0.1259	<i>R</i> ₁ = 0.0831
<i>R</i> ₁ , <i>wR</i> ₂ (all data)	<i>wR</i> ₂ = 0.1811	<i>wR</i> ₂ = 0.1943	<i>wR</i> ₂ = 0.1637
<i>S</i>	1.116	1.018	1.074
Max/min $\Delta\rho/e\text{ \AA}^{-3}$	2.885 / -2.510	1.983 / -1.212	5.007 / -2.667

$$R_1 = \sum ||F_o - |F_c|| / \sum |F_o|, wR_2 = [\sum [w(F_o^2 - F_c^2)^2] / \sum w(F_o^2)^2]^{1/2}$$

Table S2. Selected bond distances (\AA) and angles ($^\circ$) in helicates **1-Eu**, **1-Dy** and **1-Er**.

Bond distances	Bond angles		
1-Eu			
Eu1–O1	2.318(4)	O11–Eu1–O2	140.8(2)
Eu1–O2	2.284(4)	O11–Eu1–O10	68.9(1)
Eu1–O10	2.318(5)	O2–Eu1–O10	131.5(2)
Eu1–O11	2.282(4)	O11–Eu1–O1	126.9(2)
Eu1–O13	2.515(5)	O2–Eu1–O1	69.0(1)
Eu1–O17	2.517(5)	O10–Eu1–O1	131.9(2)
Eu1–N2	2.599(5)	O11–Eu1–O13	78.3(2)
Eu1–N10	2.626(5)	O2–Eu1–O13	135.4(2)
Eu2–O7	2.277(4)	O11–Eu1–O17	136.6(2)
Eu2–O8	2.307(4)	O2–Eu1–O17	77.7(2)
Eu2–O9	2.308(4)	O10–Eu1–O17	68.8(1)
Eu2–O12	2.320(5)	O1–Eu1–O17	77.8(2)
Eu2–O16	2.492(5)	O13–Eu1–O17	80.6(2)
Eu2–O18	2.512(5)	O11–Eu1–N2	89.4(2)
Eu2–N7	2.604(5)	O2–Eu1–N2	68.2(2)
Eu2–N9	2.593(5)	O10–Eu1–N2	78.0(2)
Eu3–O3	2.268(4)	O1–Eu1–N2	137.1(2)
Eu3–O4	2.337(4)	O13–Eu1–N2	150.6(2)
Eu3–O5	2.316(4)	O17–Eu1–N2	90.8(2)
Eu3–O6	2.299(4)	O11–Eu1–N10	68.1(2)
Eu3–O14	2.520(4)	O2–Eu1–N10	83.5(2)
Eu3–O15	2.507(4)	O10–Eu1–N10	136.9(2)
Eu3–N3	2.602(5)	O1–Eu1–N10	78.7(2)
Eu3–N6	2.594(6)	O13–Eu1–N10	101.0(2)
	O17–Eu1–N10	153.9(2)	
	N2–Eu1–N10	99.0(1)	
	O7–Eu2–O8	68.9(2)	
	O7–Eu2–O9	139.7(2)	
	O8–Eu2–O9	130.1(2)	
	O7–Eu2–O12	129.9(2)	
	O8–Eu2–O12	130.2(2)	
	O9–Eu2–O12	69.9(2)	
	O7–Eu2–O16	137.4(2)	
	O8–Eu2–O16	69.3(2)	
	O9–Eu2–O16	76.5(2)	
	O12–Eu2–O16	75.1(2)	
	O7–Eu2–O18	78.0(1)	
	O8–Eu2–O18	73.4(2)	

O9–Eu2–O18	137.3(2)
O12–Eu2–O18	68.7(2)
O16–Eu2–O18	83.2(2)
O7–Eu2–N9	85.0(2)
O8–Eu2–N9	78.6(2)
O9–Eu2–N9	68.6(2)
O12–Eu2–N9	138.5(1)
O16–Eu2–N9	94.1(2)
O18–Eu2–N9	151.0(2)
O7–Eu2–N7	67.9(2)
O8–Eu2–N7	136.8(2)
O9–Eu2–N7	85.1(2)
O12–Eu2–N7	80.7(1)
O16–Eu2–N7	153.4(2)
O18–Eu2–N7	98.1(2)
N9–Eu2–N7	97.0(2)
O3–Eu3–O6	140.3(2)
O3–Eu3–O5	130.1(2)
O6–Eu3–O5	68.0(2)
O3–Eu3–O4	69.0(2)
O6–Eu3–O4	129.8(2)
O5–Eu3–O4	131.9(2)
O3–Eu3–O15	135.4(2)
O6–Eu3–O15	79.4(2)
O5–Eu3–O15	74.7(2)
O4–Eu3–O15	68.1(1)
O3–Eu3–O14	78.5(2)
O6–Eu3–O14	135.4(2)
O5–Eu3–O14	68.5(2)
O4–Eu3–O14	75.8(2)
O15–Eu3–O14	79.9(2)
O3–Eu3–N6	84.1(1)
O6–Eu3–N6	67.9(2)
O5–Eu3–N6	135.7(2)
O4–Eu3–N6	81.9(2)
O15–Eu3–N6	101.3(2)
O14–Eu3–N6	155.5(2)
O3–Eu3–N3	68.3(1)
O6–Eu3–N3	85.9(2)
O5–Eu3–N3	78.2(2)
O4–Eu3–N3	137.3(2)

	O15–Eu3–N3	152.4(2)	
	O14–Eu3–N3	94.9(2)	
	N6–Eu3–N3	94.5(2)	
<hr/>			
1-Dy			
Dy1–O7	2.252(6)	O7–Dy1–O7	141.4(3)
Dy1–O8	2.260(6)	O7–Dy1–O8	68.7(2)
Dy1–O9	2.496(8)	O7–Dy1–O9	76.3(2)
Dy1–N5	2.546(7)	O8–Dy1–O8	133.2(3)
Dy2–O1	2.304(6)	O8–Dy1–O9	77.7(2)
Dy2–O2	2.235(6)	O9–Dy1–O9	85.9(4)
Dy2–O3	2.274(6)	O7–Dy1–N5	69.7(2)
Dy2–O4	2.227(6)	O8–Dy1–N5	138.3(2)
Dy2–O5	2.506(6)	O9–Dy1–N5	94.1(3)
Dy2–O6	2.461(6)	N5–Dy1–N5	98.2(3)
Dy2–N2	2.512(8)	O4–Dy2–O2	142.3(2)
Dy2–N4	2.583(7)	O4–Dy2–O3	70.3(2)
		O2–Dy2–O3	128.2(2)
		O4–Dy2–O1	125.1(2)
		O2–Dy2–O1	70.4(2)
		O3–Dy2–O1	132.3(2)
		O4–Dy2–O6	138.5(2)
		O2–Dy2–O6	75.1(2)
		O3–Dy2–O6	70.1(2)
		O1–Dy2–O6	75.9(2)
		O4–Dy2–O5	76.0(2)
		O2–Dy2–O5	137.0(2)
		O3–Dy2–O5	73.0(2)
		O1–Dy2–O5	69.4(2)
		O6–Dy2–O5	81.0(2)
		O4–Dy2–N2	86.9(2)
		O2–Dy2–N2	69.7(2)
		O3–Dy2–N2	77.0(2)
		O1–Dy2–N2	140.0(2)
		O6–Dy2–N2	96.0(2)
		O5–Dy2–N2	149.0(2)
		O4–Dy2–N4	68.1(2)
		O2–Dy2–N4	83.1(2)
		O3–Dy2–N4	137.4(2)
		O1–Dy2–N4	81.2(2)
		O6–Dy2–N4	152.5(2)
		O5–Dy2–N4	104.9(2)

		N2–Dy2–N4	91.9(2)
1-Er			
Er1–O8	2.238(5)	O8–Er1–O8	133.5(3)
Er1–O7	2.241(4)	O8–Er1–O7	68.5(2)
Er1–O9	2.483(5)	O7–Er1–O7	141.2(2)
Er1–N5	2.526(6)	O8–Er1–O9	77.2(2)
Er2–O1	2.279(5)	O7–Er1–O9	76.1(2)
Er2–O2	2.217(5)	O9–Er1–O9	85.9(3)
Er2–O3	2.253(5)	O8–Er1–N5	138.6(1)
Er2–O4	2.219(5)	O7–Er1–N5	70.1(2)
Er2–O5	2.458(5)	O9–Er1–N5	95.1(2)
Er2–O6	2.435(5)	N5–Er1–N5	97.0(3)
Er2–N2	2.516(6)	O2–Er2–O4	142.3(2)
Er2–N4	2.558(6)	O2–Er2–O3	127.5(2)
		O4–Er2–O3	70.5(2)
		O2–Er2–O1	70.8(1)
		O4–Er2–O1	125.6(2)
		O3–Er2–O1	131.8(2)
		O2–Er2–O6	74.9(2)
		O4–Er2–O6	139.1(2)
		O3–Er2–O6	71.0(2)
		O1–Er2–O6	73.7(1)
		O2–Er2–O5	138.3(1)
		O4–Er2–O5	74.9(2)
		O3–Er2–O5	73.2(2)
		O1–Er2–O5	69.9(2)
		O6–Er2–O5	81.2(2)
		O2–Er2–N2	70.4(2)
		O4–Er2–N2	85.2(2)
		O3–Er2–N2	77.0(1)
		O1–Er2–N2	141.0(2)
		O6–Er2–N2	99.2(2)
		O5–Er2–N2	148.2(2)
		O2–Er2–N4	82.7(2)
		O4–Er2–N4	69.4(2)
		O3–Er2–N4	139.1(2)
		O1–Er2–N4	80.0(2)
		O6–Er2–N4	149.8(2)
		O5–Er2–N4	103.6(1)
		N2–Er2–N4	91.9(2)

Table S3. Hydrogen bonding parameters (\AA , $^\circ$) in helicates **1-Eu**, **1-Dy** and **1-Er**.

D–H···A	D–H	H···A	D···A	$\angle\text{DHA}$
1-Eu				
O2–H2A···O1	0.99	2.12	2.605(7)	108
O2–H2A···N1	0.99	1.75	2.688(7)	157
O4–H4A···O3	0.99	2.09	2.610(6)	111
O4–H4A···N4	0.99	1.85	2.747(7)	150
O5–H5A···O6	0.99	2.04	2.580(6)	112
O5–H5A···N5	0.99	1.83	2.736(7)	150
O7–H7A···O8	0.99	2.10	2.592(6)	108
O7–H7A···N8	0.99	1.75	2.699(7)	160
O8–H8C···N9	0.99	2.59	3.113(6)	113
O11–H11H···O10	0.99	2.08	2.601(6)	110
O11–H11H···N11	0.99	1.76	2.704(7)	157
1-Dy				
O2–H2A···O1	0.97	2.12	2.618(8)	110
O2–H2A···N1	0.97	1.77	2.704(8)	160
O4–H4A···O5	0.97	2.40	2.923(8)	113
O4–H4A···N3	0.97	1.84	2.651(9)	139
1-Er				
O2–H2A···O1	0.97	2.14	2.604(8)	108
O2–H2A···N1	0.97	1.75	2.681(8)	160
O4–H4A···O5	0.97	2.37	2.851(7)	110
O4–H4A···N3	0.97	1.79	2.629(8)	143

Figures:

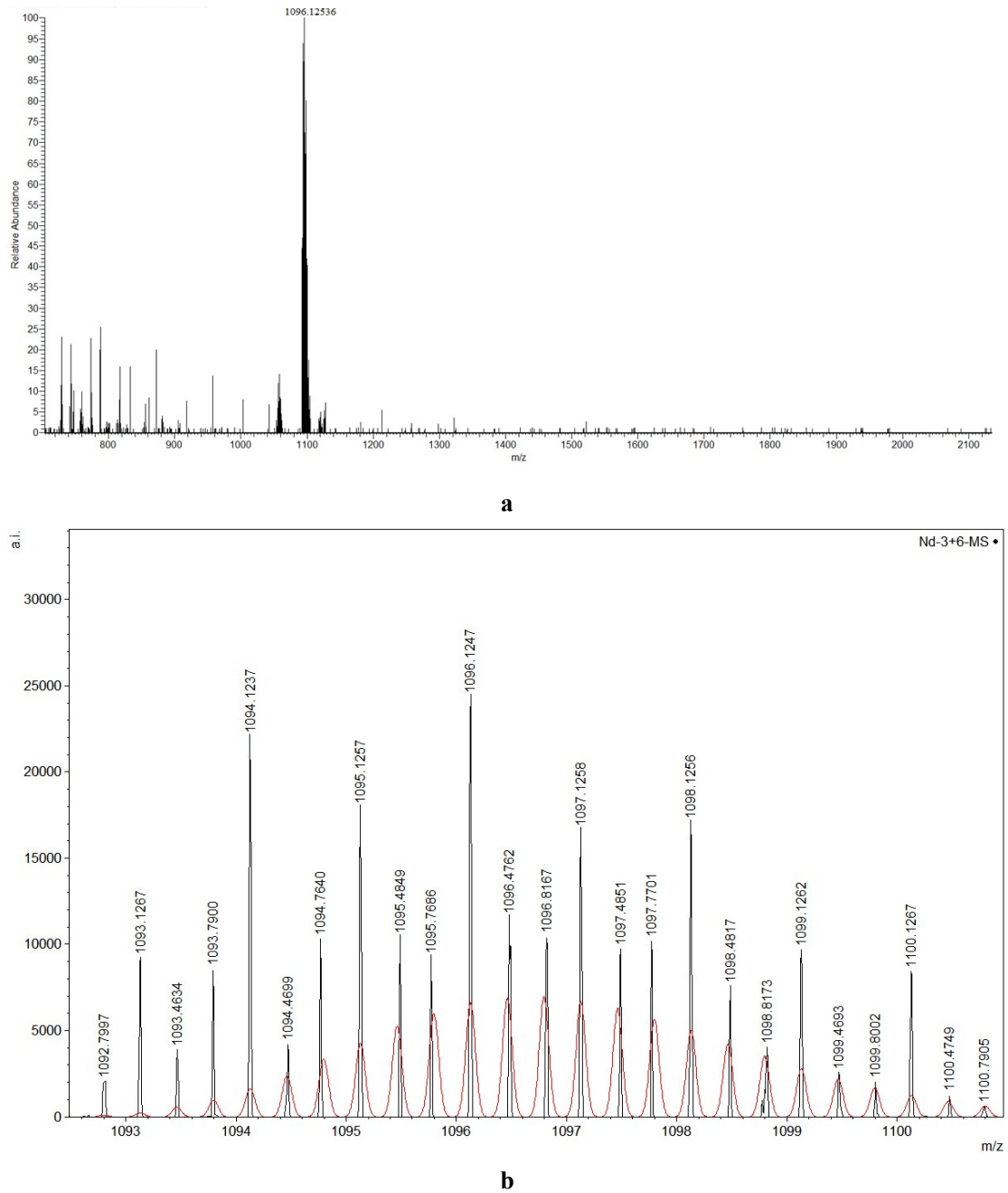
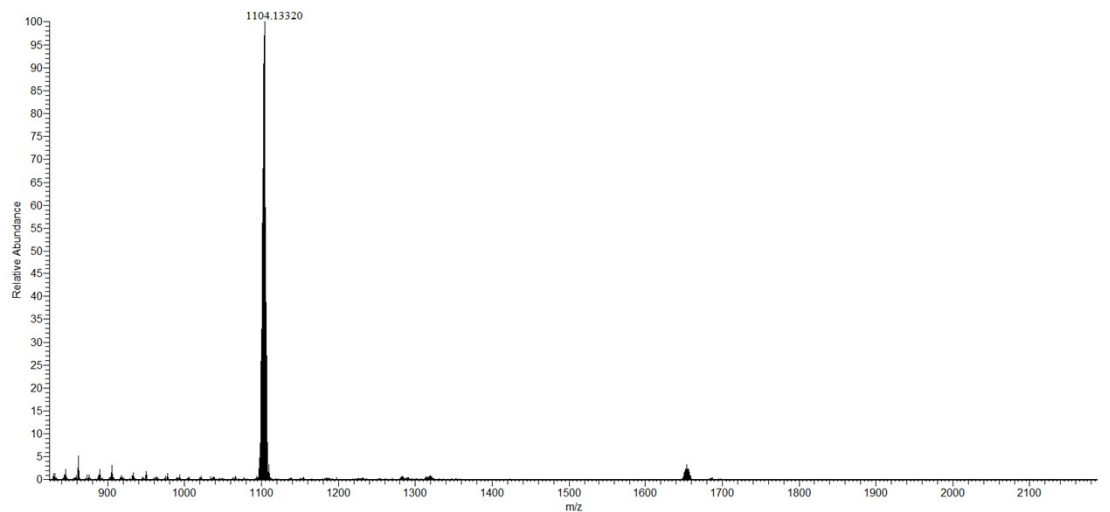
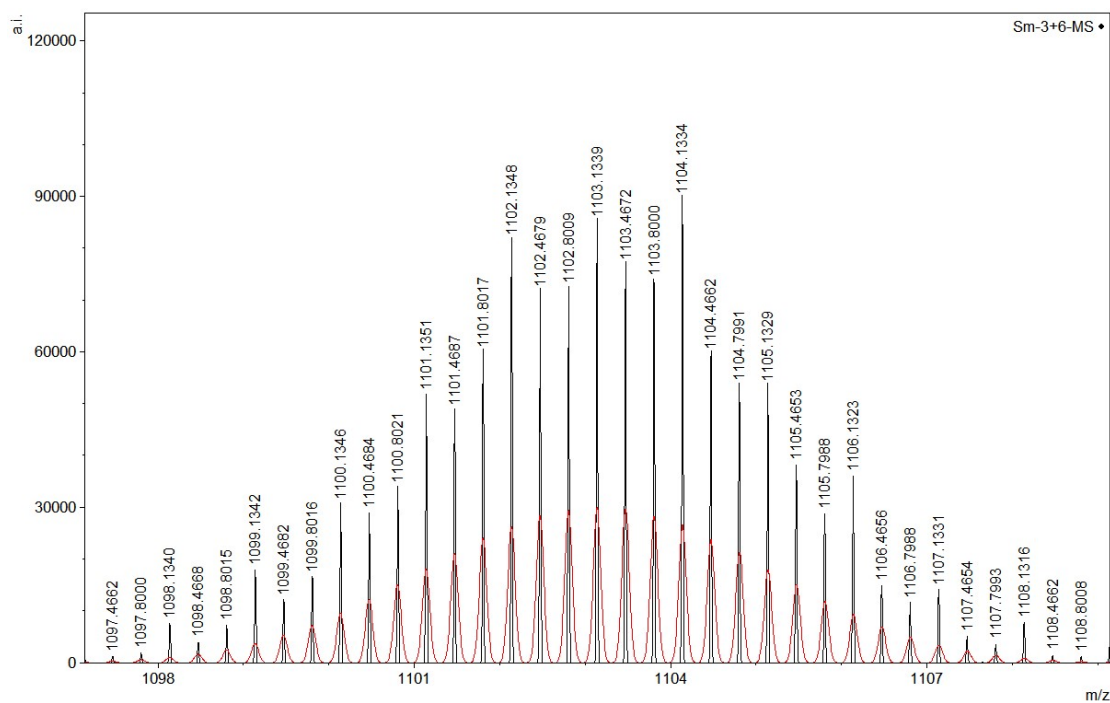


Fig. S1. (a) High-resolution ESI-mass spectrometry analysis of $[Nd_3L_3]^{3+}$; (b) Experimental (black line) and calculated isotopic distribution (red line) for comparison.

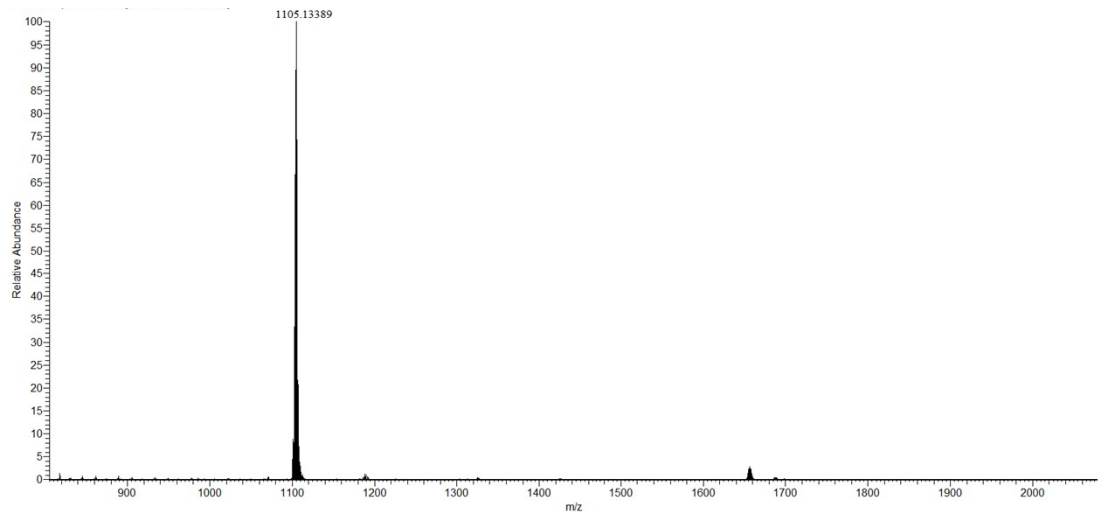


a

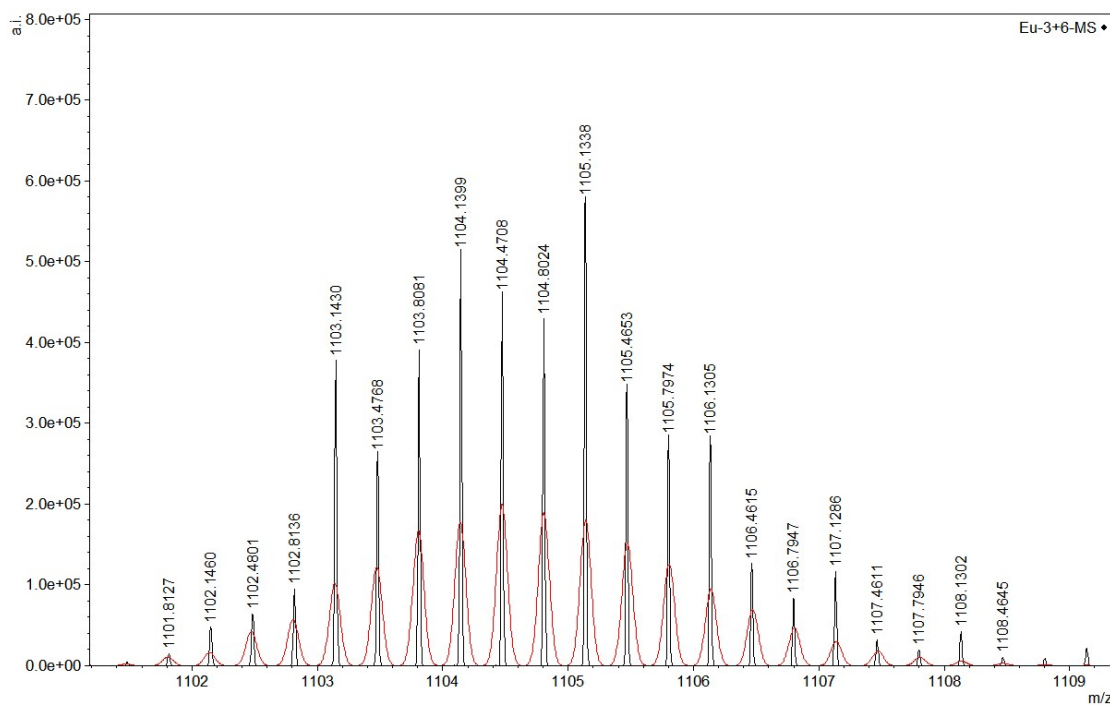


b

Fig. S2. (a) High-resolution ESI-mass spectrometry analysis of $[Sm_3L_3]^{3+}$; (b) Experimental (black line) and calculated isotopic distribution (red line) for comparison.



a



b

Fig. S3. (a) High-resolution ESI-mass spectrometry analysis of $[\text{Eu}_3\text{L}_3]^{3+}$; (b) Experimental (black line) and calculated isotopic distribution (red line) for comparison.

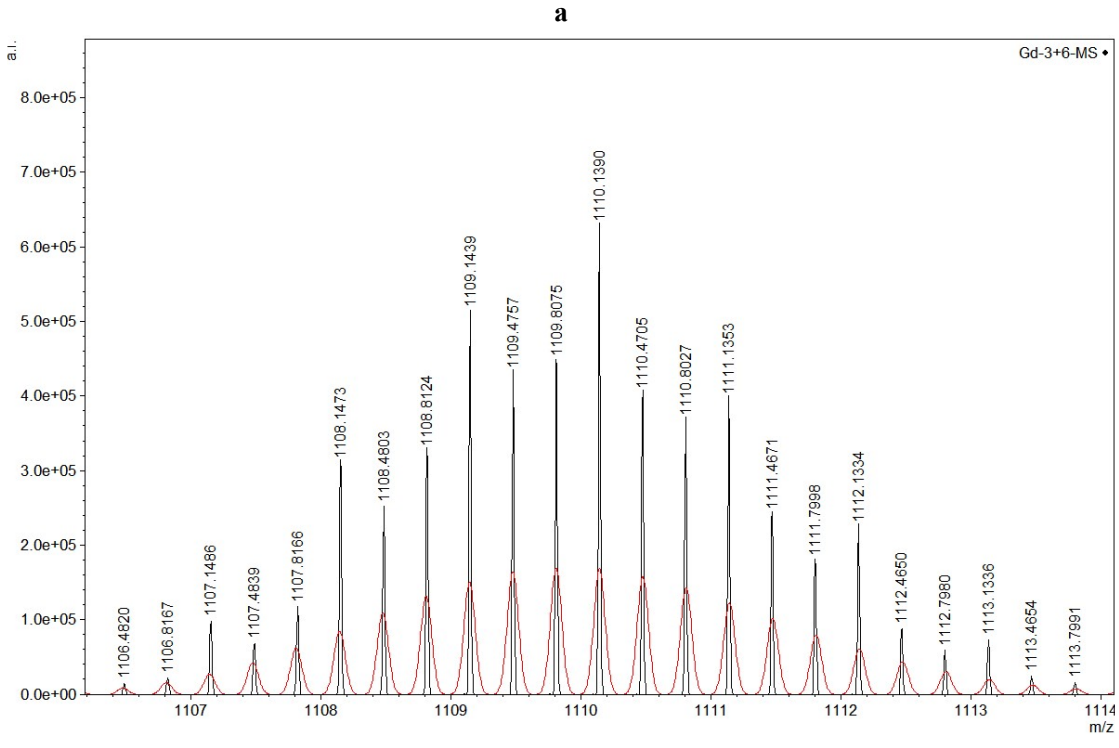
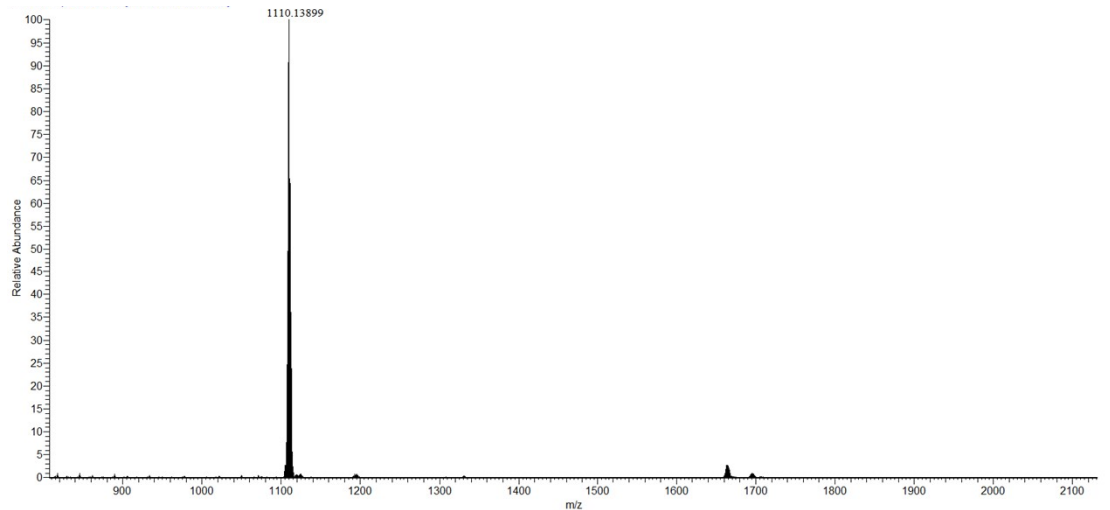
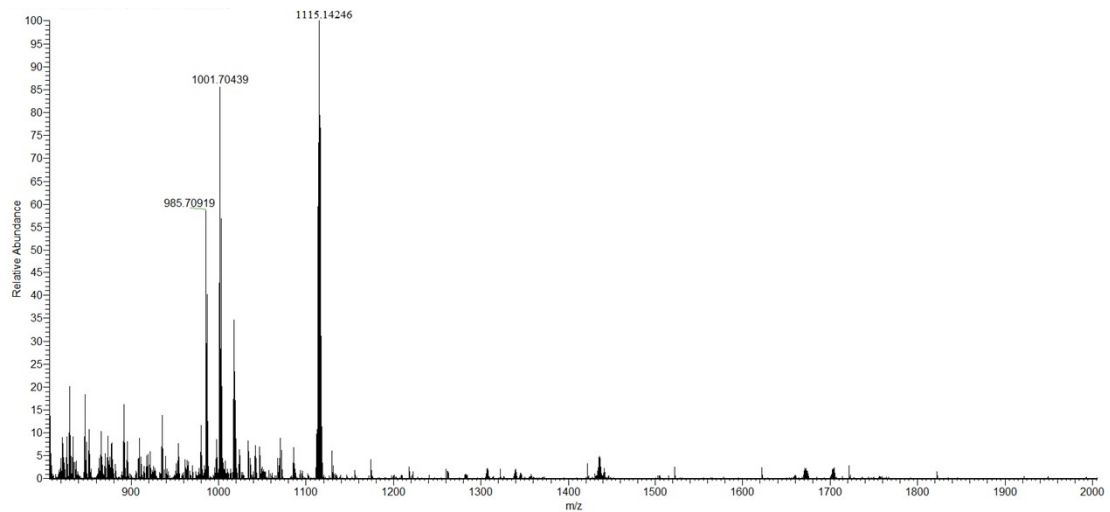


Fig. S4. (a) High-resolution ESI-mass spectrometry analysis of $[Gd_3L_3]^{3+}$; (b) Experimental (black line) and calculated isotopic distribution (red line) for comparison.



a

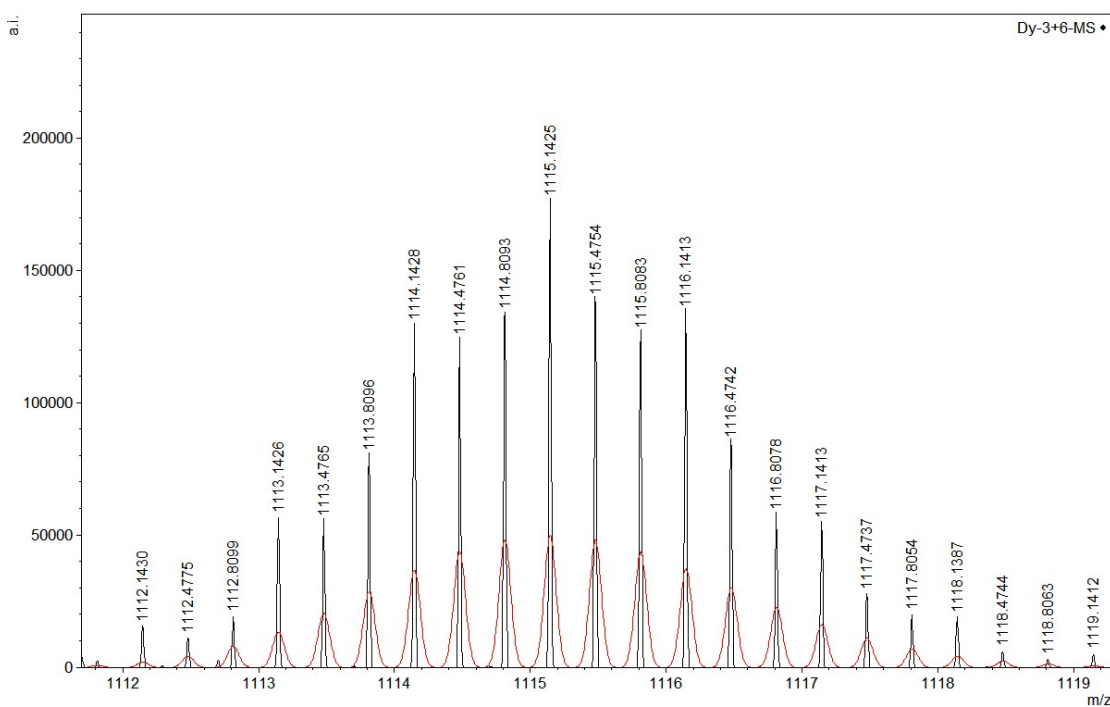
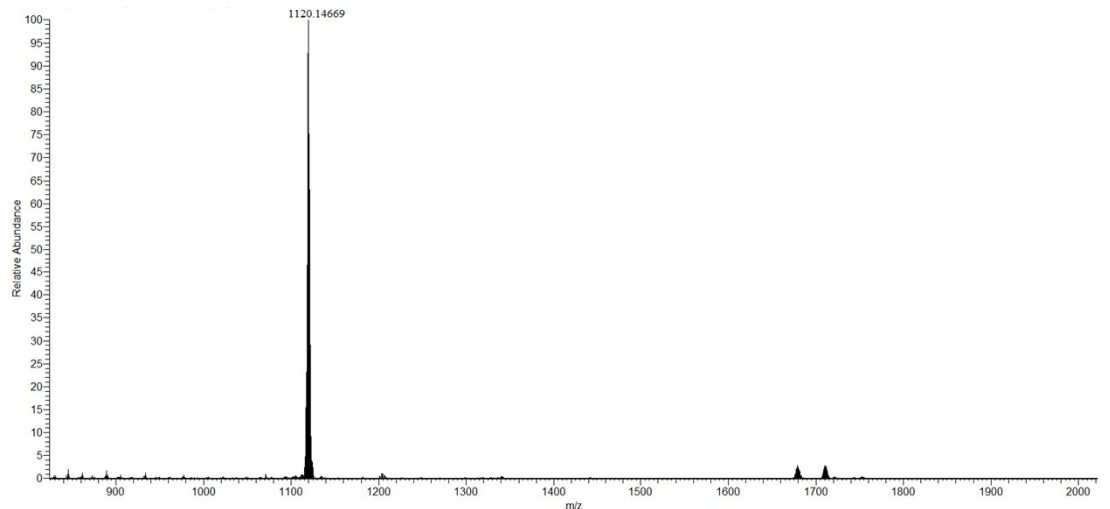
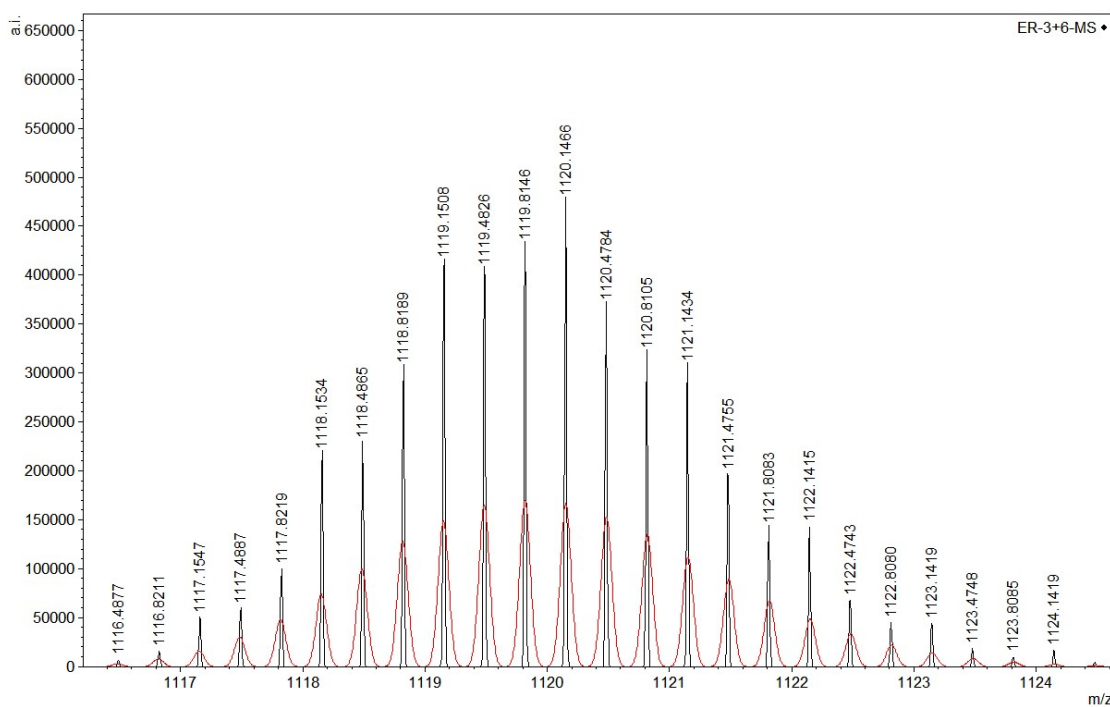


Fig. S5. (a) High-resolution ESI-mass spectrometry analysis of $[Dy_3L_3]^{3+}$; (b) Experimental (black line) and calculated isotopic distribution (red line) for comparison.



a



b

Fig. S6. (a) High-resolution ESI-mass spectrometry analysis of $[Er_3L_3]^{3+}$; (b) Experimental (black line) and calculated isotopic distribution (red line) for comparison.

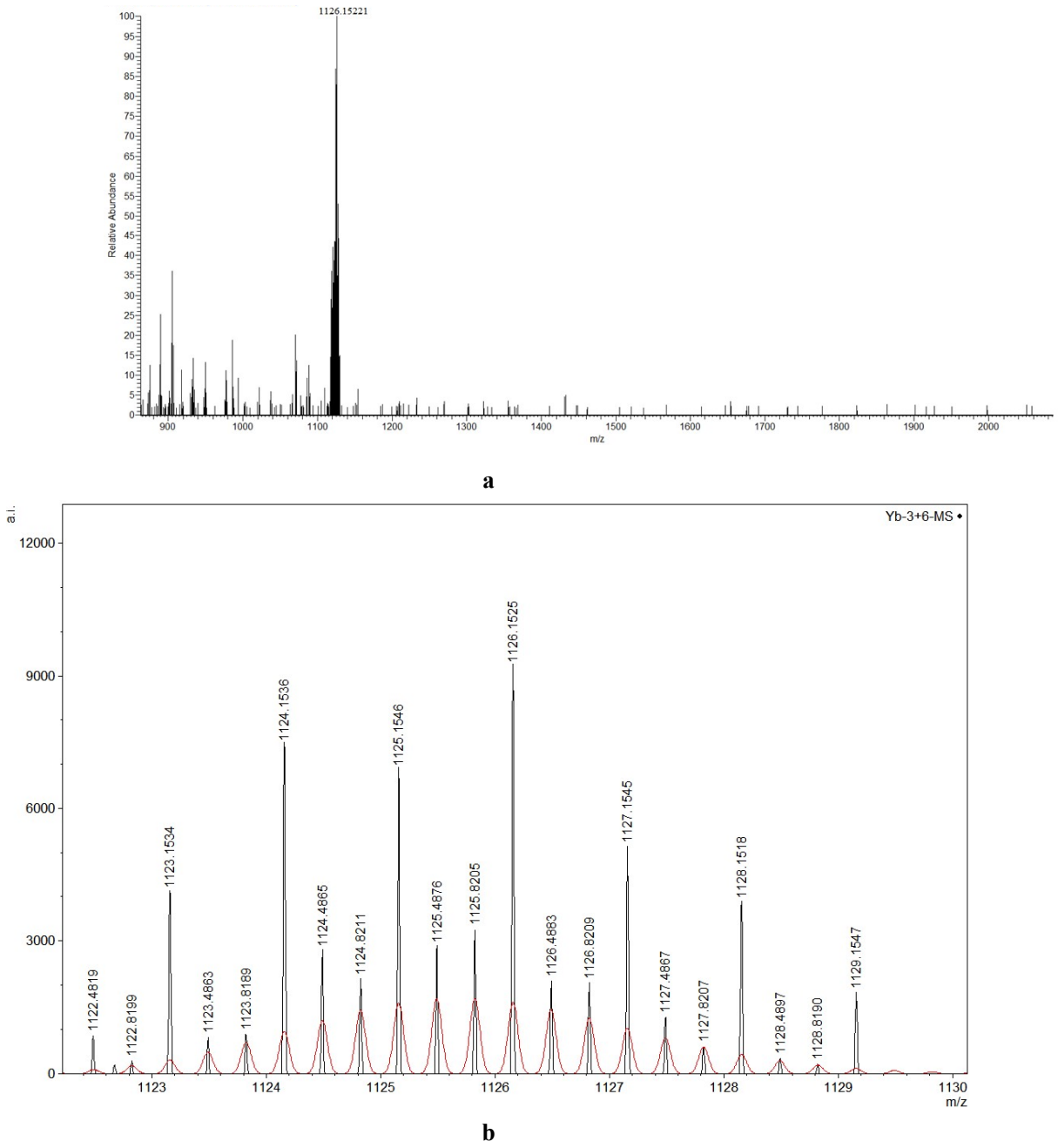


Fig. S7. (a) High-resolution ESI-mass spectrometry analysis of $[Yb_3L_3]^{3+}$; (b) Experimental (black line) and calculated isotopic distribution (red line) for comparison.

Ion Series			
Σ	O_2^-	M^+	Formula: <chem>(C51H46CHN4O6)3Nd3Cl3</chem>
Agent:	Cl	Agent charge:	-1
Polarity:	<input checked="" type="radio"/> Positive	<input type="radio"/> Negative	
ion	monoisotopic mass	average mass	
[M]	3381.2812	3397.3051	
[M-1Cl] 1+	3346.3118	3361.8520	
[M-2Cl] 2+	1655.6712	1663.1995	
[M-3Cl] 3+	1092.1243	1096.9819	
Σ	O_2^-	M^+	Formula: <chem>(C51H46CHN4O6)3Sm3Cl3</chem>
Agent:	Cl	Agent charge:	-1
Polarity:	<input checked="" type="radio"/> Positive	<input type="radio"/> Negative	
ion	monoisotopic mass	average mass	
[M]	3411.3172	3415.6957	
[M-1Cl] 1+	3376.3478	3380.2426	
[M-2Cl] 2+	1670.6892	1672.3948	
[M-3Cl] 3+	1102.1363	1103.1122	
Σ	O_2^-	M^+	Formula: <chem>(C51H46CHN4O6)3Eu3Cl3</chem>
Agent:	Cl	Agent charge:	-1
Polarity:	<input checked="" type="radio"/> Positive	<input type="radio"/> Negative	
ion	monoisotopic mass	average mass	
[M]	3414.3217	3420.4898	
[M-1Cl] 1+	3379.3523	3385.0367	
[M-2Cl] 2+	1672.1914	1674.7918	
[M-3Cl] 3+	1103.1378	1104.7102	
Σ	O_2^-	M^+	Formula: <chem>(C51H46CHN4O6)3Gd3Cl3</chem>
Agent:	Cl	Agent charge:	-1
Polarity:	<input checked="" type="radio"/> Positive	<input type="radio"/> Negative	
ion	monoisotopic mass	average mass	
[M]	3429.3303	3436.3531	
[M-1Cl] 1+	3394.3609	3400.9000	
[M-2Cl] 2+	1679.6957	1682.7234	
[M-3Cl] 3+	1108.1407	1109.9979	
Σ	O_2^-	M^+	Formula: <chem>(C51H46CHN4O6)3Dy3Cl3</chem>
Agent:	Cl	Agent charge:	-1
Polarity:	<input checked="" type="radio"/> Positive	<input type="radio"/> Negative	
ion	monoisotopic mass	average mass	
[M]	3447.3455	3452.0878	
[M-1Cl] 1+	3412.3761	3416.6347	
[M-2Cl] 2+	1688.7034	1690.5908	
[M-3Cl] 3+	1114.1458	1115.2428	
Σ	O_2^-	M^+	Formula: <chem>(C51H46CHN4O6)3Er3Cl3</chem>
Agent:	Cl	Agent charge:	-1
Polarity:	<input checked="" type="radio"/> Positive	<input type="radio"/> Negative	
ion	monoisotopic mass	average mass	
[M]	3453.3489	3466.3656	
[M-1Cl] 1+	3418.3795	3430.9125	
[M-2Cl] 2+	1691.7050	1697.7297	
[M-3Cl] 3+	1116.1469	1120.0021	
Σ	O_2^-	M^+	Formula: <chem>(C51H46CHN4O6)3Yb3Cl3</chem>
Agent:	Cl	Agent charge:	-1
Polarity:	<input checked="" type="radio"/> Positive	<input type="radio"/> Negative	
ion	monoisotopic mass	average mass	
[M]	3477.3746	3483.7098	
[M-1Cl] 1+	3442.4052	3448.2567	
[M-2Cl] 2+	1703.7179	1706.4018	
[M-3Cl] 3+	1124.1555	1125.7835	

Fig. S8. Calculated mass-spectrometry data of helicates **1**.

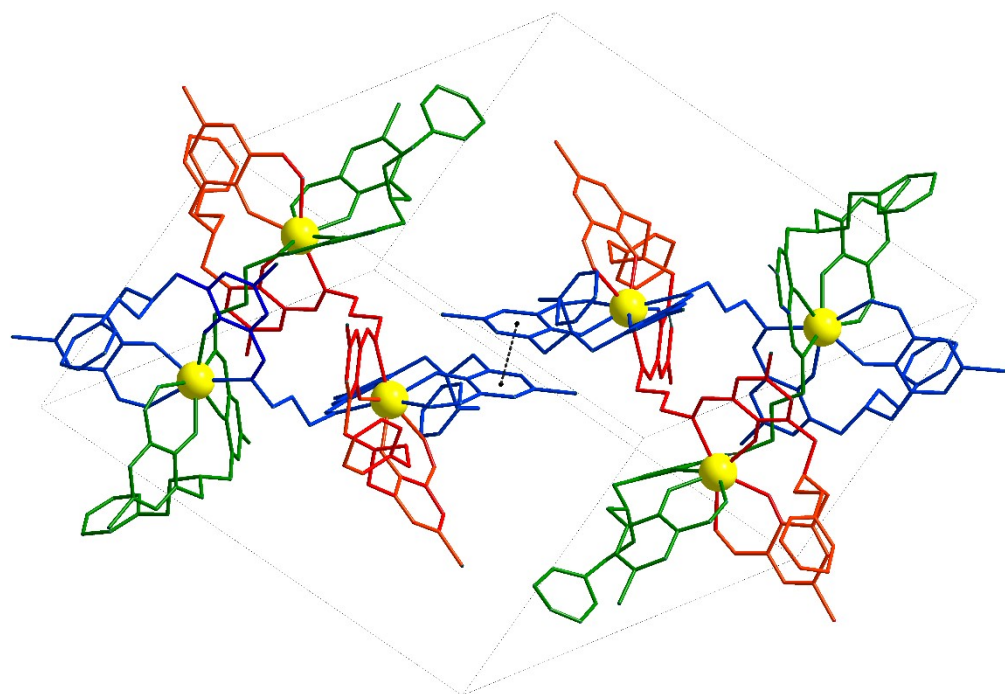


Fig. S9. Packing structure for **1-Eu**.

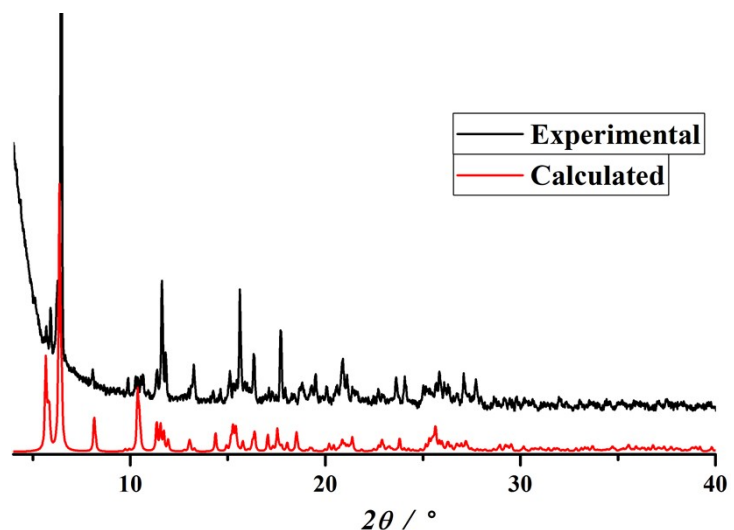


Fig. S10. Powder XRD patterns of complex **1-Nd**.

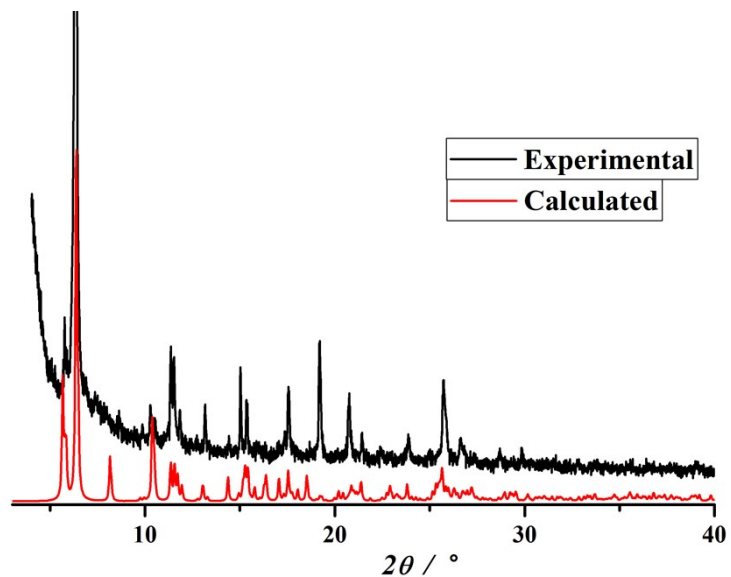


Fig. S11. Powder XRD patterns of complex **1-Sm**.

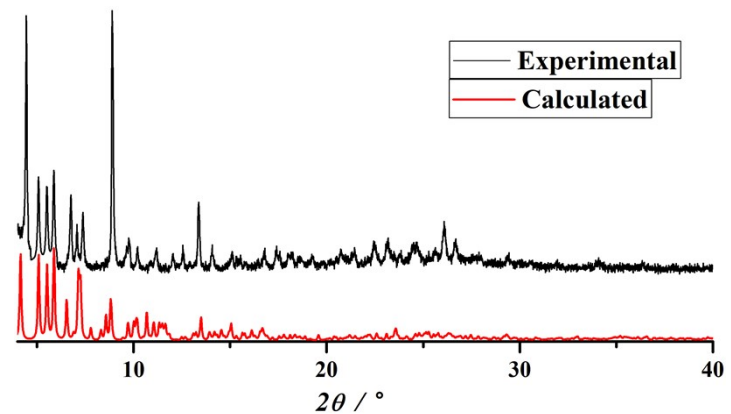


Fig. S12. Powder XRD patterns of complex **1-Eu**.

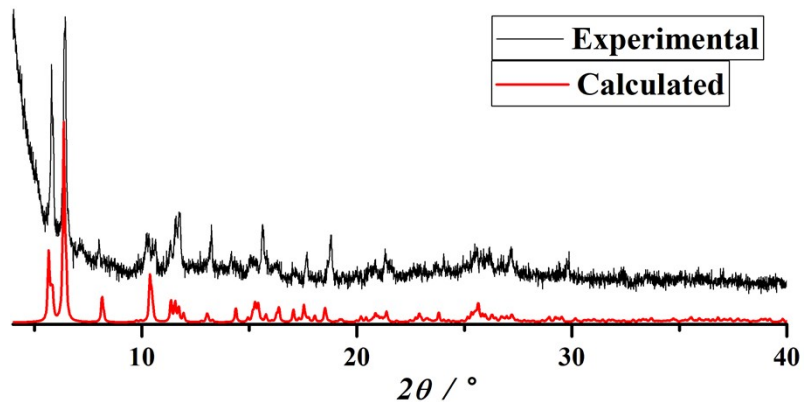


Fig. S13. Powder XRD patterns of complex **1-Gd**.

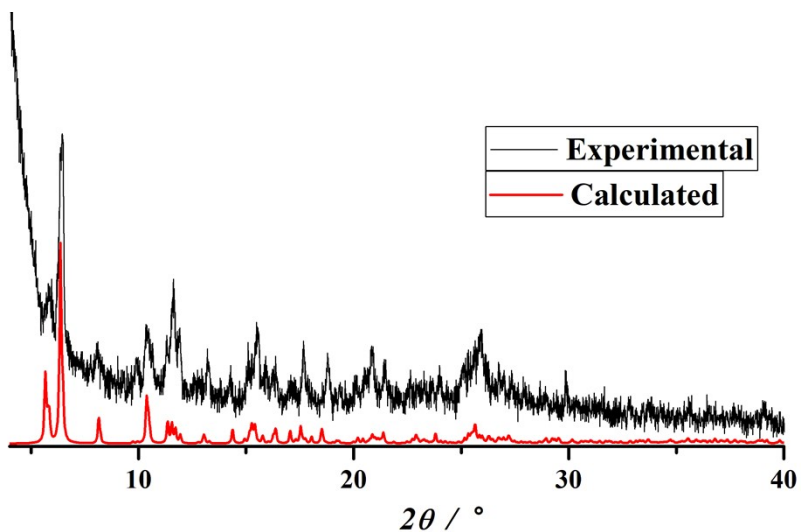


Fig. S14. Powder XRD patterns of complex 1-Dy.

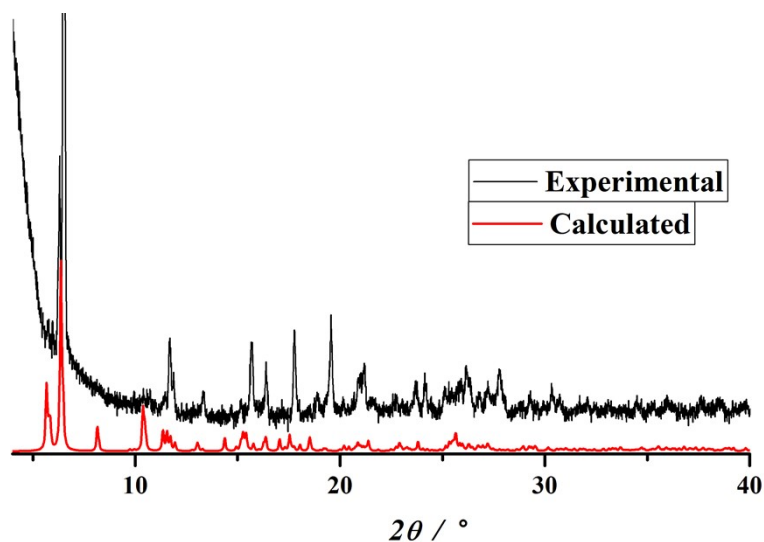


Fig. S15. Powder XRD patterns of complex 1-Er.

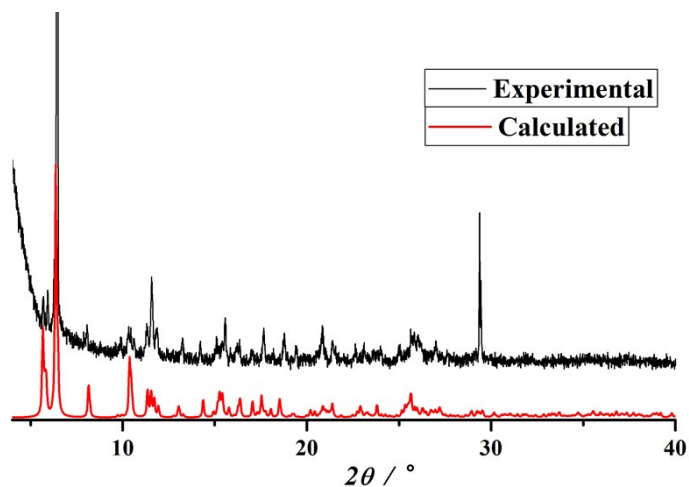


Fig. S16. Powder XRD patterns of complex 1-Yb.

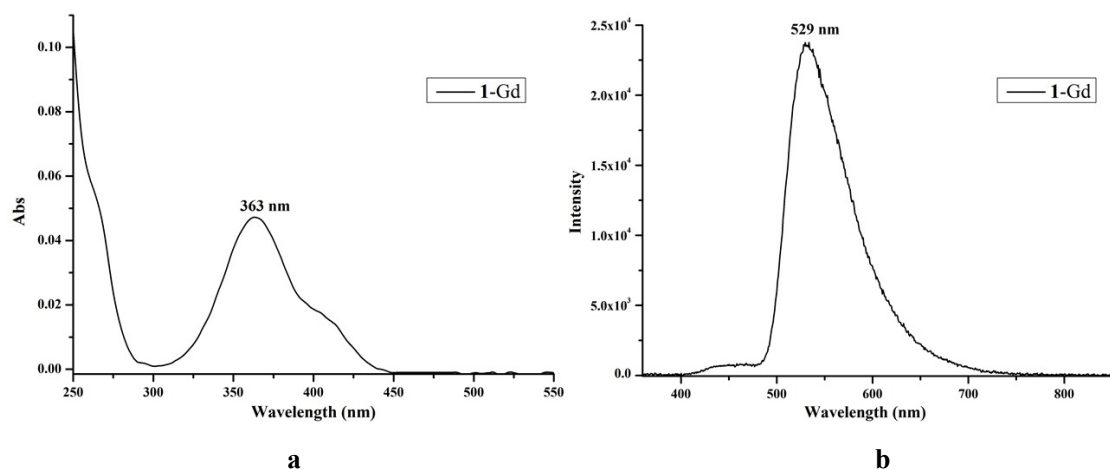


Fig. S17. (a) UV-vis absorption spectrum of complex **1**-Gd in CH_3OH ($3.5 \mu\text{M}$) at 298 K. (b) Phosphorescence emission of complex **1**-Gd based on the circular helical ligand in the solid state at 77 K.

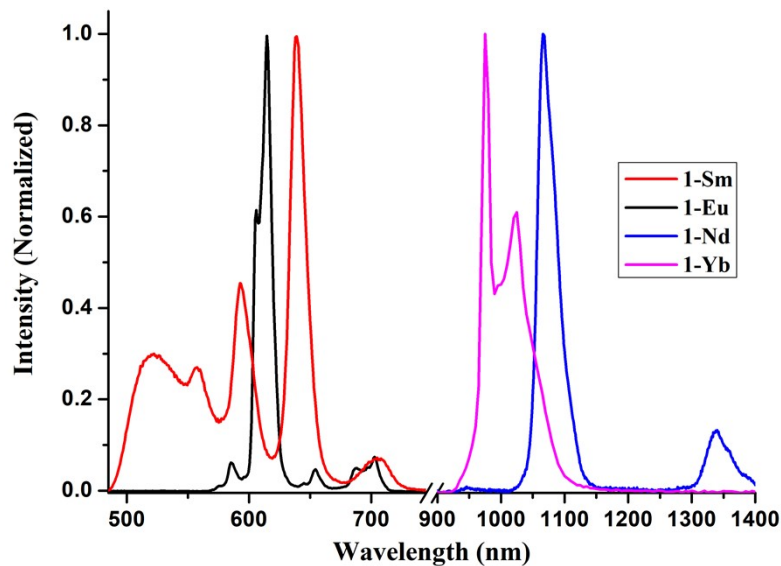


Fig. S18. Fluorescence emission spectra of helicates **1**-Sm, **1**-Eu, **1**-Nd and **1**-Yb in solid at room temperature ($\lambda_{\text{ex}} = 363 \text{ nm}$).

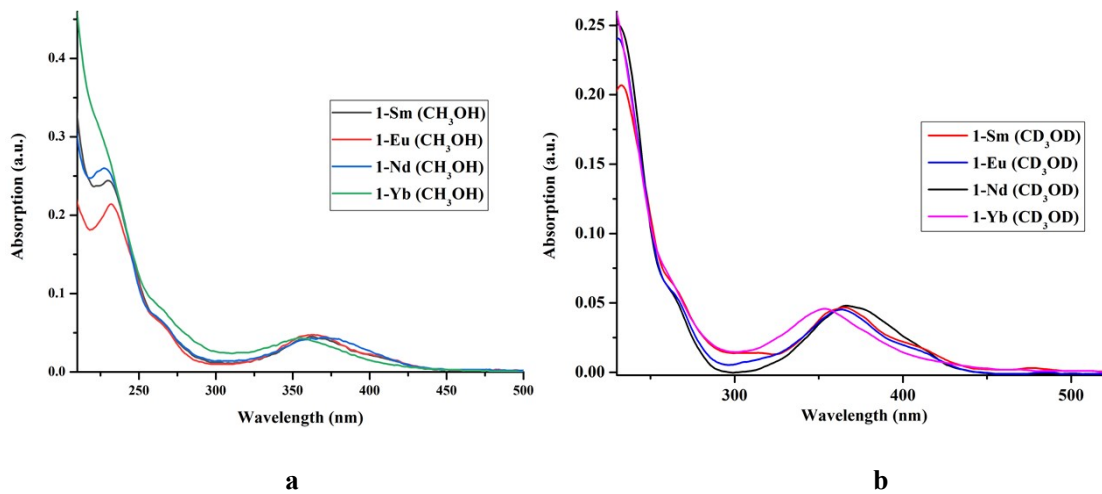


Fig. S19. UV-vis absorption spectrum of complex **1-Sm**, **1-Eu**, **1-Nd** and **1-Yb** in **a)** CH_3OH ($[\text{M}] = 3.5 \mu\text{M}$); **b)** in CD_3OD ($[\text{M}] = 3.5 \mu\text{M}$) at 298 K.

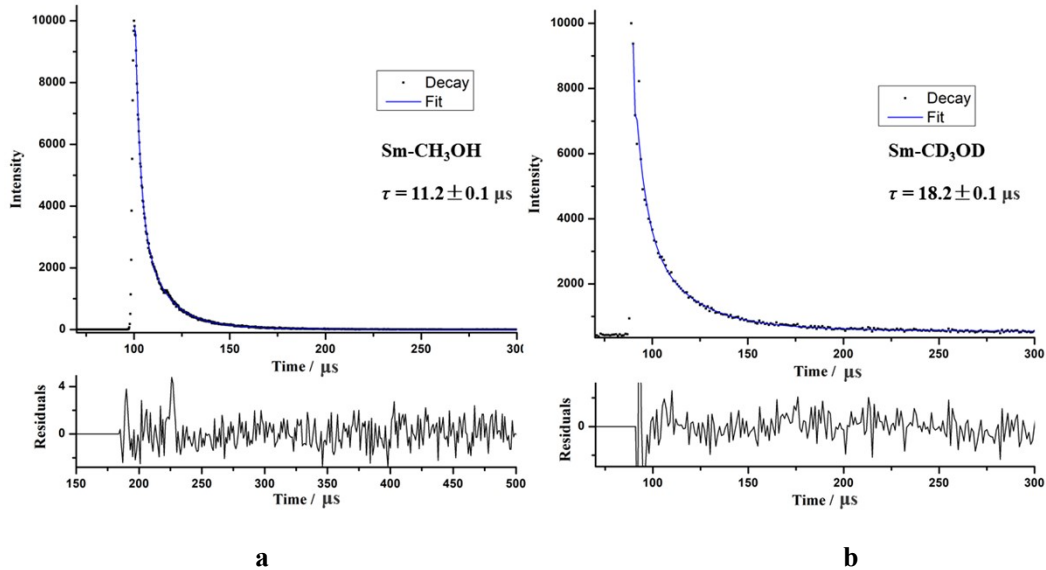


Fig. S20. Lifetimes of fluorescence measured by monitoring the emission at $\lambda_{\text{em}} = 644 \text{ nm}$. **a)** complex **1-Sm** in CH_3OH ($[\text{M}] = 3.5 \mu\text{M}$); **b)** in CD_3OD ($[\text{M}] = 3.5 \mu\text{M}$).

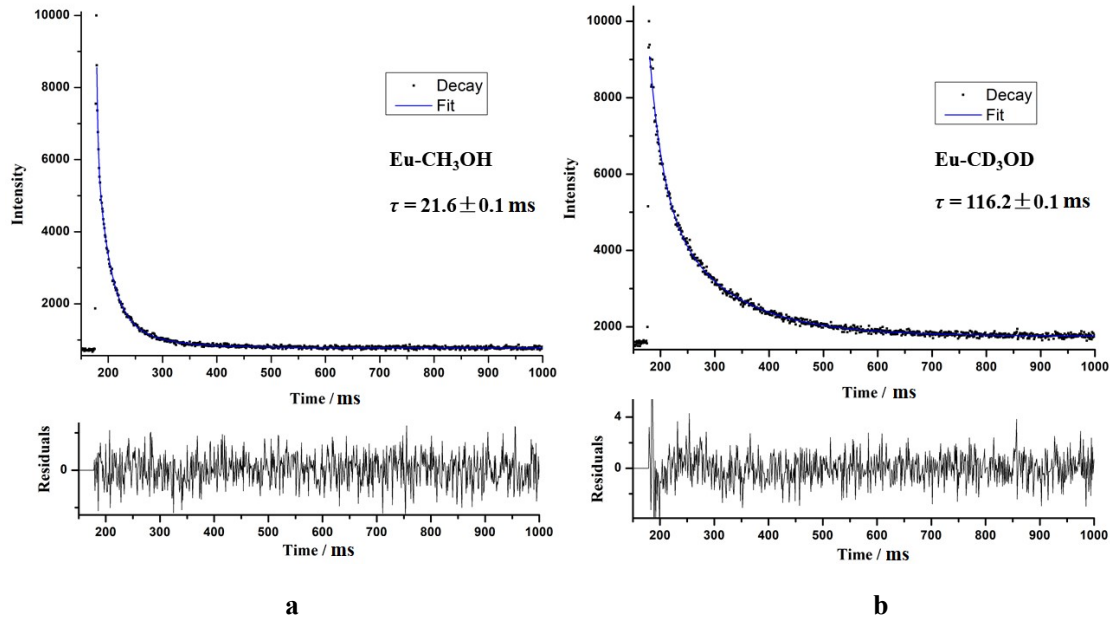


Fig. S21. Lifetimes of fluorescence measured by monitoring the emission at $\lambda_{\text{em}} = 614 \text{ nm}$. **a)** complex **1-Eu** in CH_3OH ($[M] = 3.5 \mu\text{M}$); **b)** in CD_3OD ($[M] = 3.5 \mu\text{M}$).

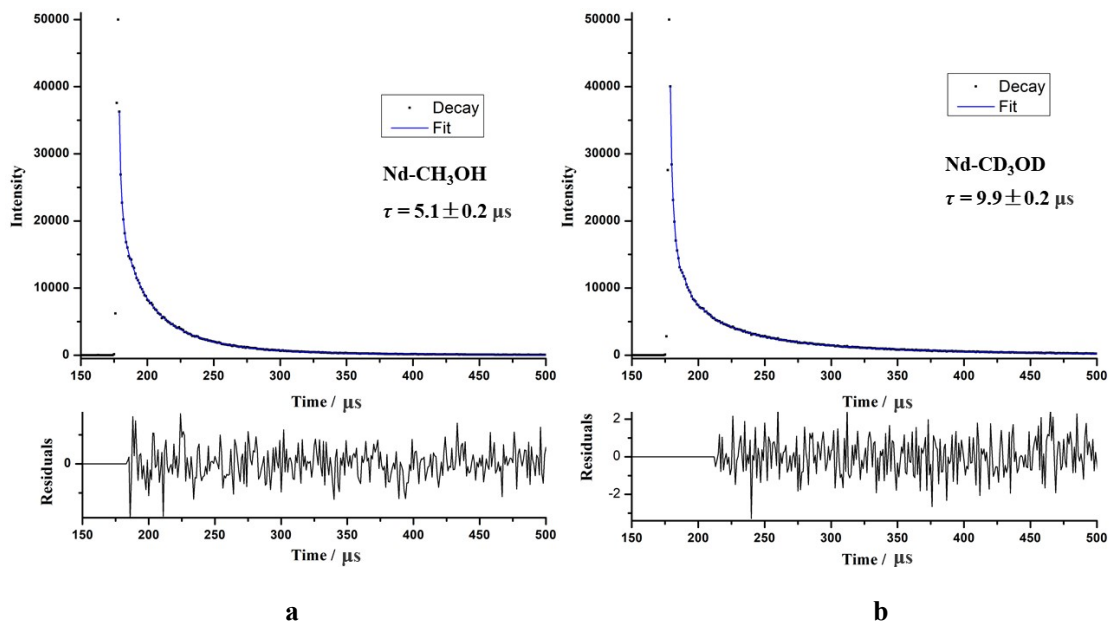


Fig. S22. Lifetimes of fluorescence measured by monitoring the emission at $\lambda_{\text{em}} = 1066 \text{ nm}$. **a)** complex **1-Nd** in CH_3OH ($[M] = 3.5 \mu\text{M}$); **b)** in CD_3OD ($[M] = 3.5 \mu\text{M}$).

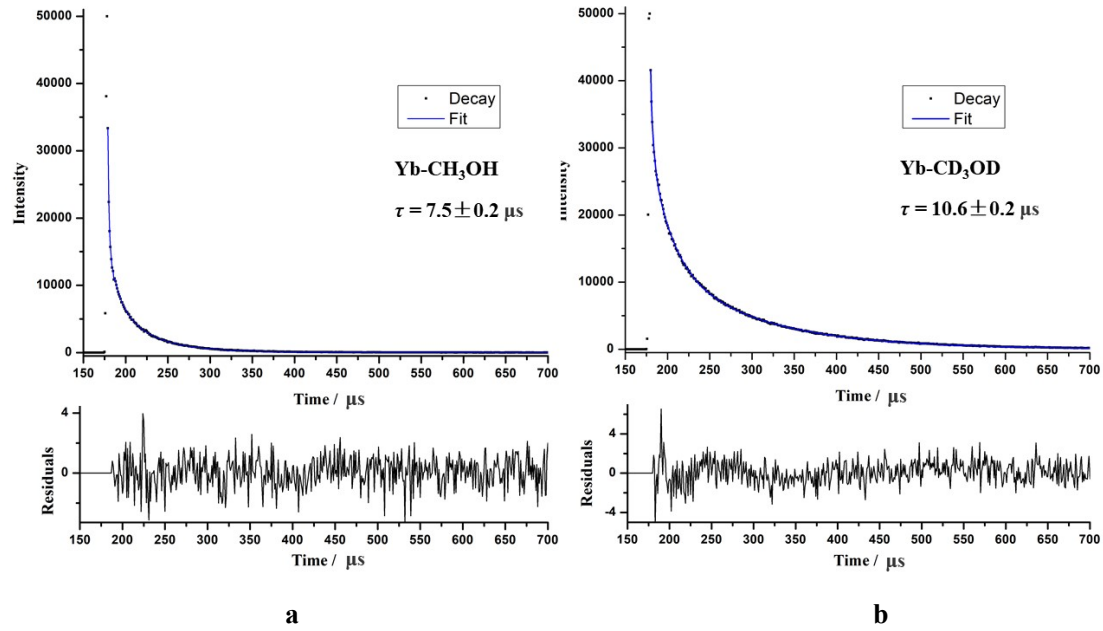


Fig. S23. Lifetimes of fluorescence measured by monitoring the emission at $\lambda_{\text{em}} = 983$ nm. **a)** complex **1**-Yb in CH₃OH ([M] = 3.5 μ M); **b)** in CD₃OD ([M] = 3.5 μ M).